

Departures from the FLRW Cosmological Model in an Inhomogeneous Universe: A Numerical Examination

John T. Giblin, Jr.^{1,2}, James B. Mertens², and Glenn D. Starkman²

¹*Department of Physics, Kenyon College, 201 N College Rd, Gambier, OH 43022 and*

²*CERCA/ISO, Department of Physics, Case Western Reserve University, 10900 Euclid Avenue, Cleveland, OH 44106*

While the use of numerical general relativity for modeling astrophysical phenomena and compact objects is commonplace, the application to cosmological scenarios is only just beginning. Here, we examine the expansion of a spacetime using the Baumgarte-Shapiro-Shibata-Nakamura (BSSN) formalism of numerical relativity in synchronous gauge. The universe that emerges exhibits an average Friedmann-Lemaître-Robertson-Walker (FLRW) behavior, however this universe also exhibits locally inhomogeneous expansion beyond that expected in linear perturbation theory around a FLRW background. This departure from FLRW is an important path-dependent effect that will need to be considered for precise calculations of physical observables in an inhomogeneous universe.

In the past two decades, numerical general relativity (GR) has been widely applied to astrophysical compact objects. Simulations of neutron stars and black holes [1–3] and, very recently, scalar fields [4], have provided answers to old questions about gravity. The success of the BSSN formalism in stabilizing error growth in numerical GR has made it a standard by which numerical GR results are measured [5].

On the other hand, current cosmological work typically relies on either a perturbative approach or a Newtonian gravity approximation. Such work has provided highly precise simulations and resolved how non-linear structure emerges. These simulations – as in almost all cosmology – rely on a flat, FLRW, cosmological background; it is commonly assumed that any sub-horizon inhomogeneous structure of the Universe will contribute to an average expansion of the Universe on horizon-sized volumes driven by the horizon-averaged density. When photons are then propagated through the simulated universe, they are red-shifted according to the homogeneous FLRW expansion and corrections from Sachs-Wolfe effects.

Such simplified averaging assumptions have long been a matter of concern, and have often been questioned (for a recent review, see [6]). However, for practical reasons these assumptions have been relaxed in favor of idealized or simplified contexts (eg. [7–11]). The object of this investigation is to begin to move that evaluation, and the quantification of the consequent inaccuracy or imprecision of our cosmological inferences, into a fully general-relativistic setting.

The BSSN formalism [12, 13] is a modification of the ADM Hamiltonian formalism [14] of general relativity designed to improve the numerical stability of the latter by introducing auxiliary variables. The equations that define the BSSN formalism are nonlinear, and therefore formidable to work with analytically. Nevertheless, the nonlinear terms are few enough that – depending on gauge choice – numerically integrating the fully unconstrained Einstein equations does not require significantly more computing resources than working in a linearized

gravity regime.

In this letter, we study a space-time in which inhomogeneities are present at a range of scales. We set FLRW-like initial conditions – that is, we include density inhomogeneities (with a range of power spectrum amplitudes) on top of a slice of the FLRW metric of constant extrinsic curvature. We then evolve the complete BSSN dynamical system in the full non-linear framework of GR, without assuming a background solution. As the simulation progresses, we monitor the consistency of the usual FLRW approximation in two ways: (1) observing how well the evolution of the fields corresponds to linearized theory, and (2) observing how well the average expansion rate corresponds to expectations for the background.

The software we have developed to simulate cosmological scenarios in full numerical relativity, COSMOGRAPH, has passed a standard set of tests and is able to evolve more scenarios than those presented here. For more information about these tests, the full implementation of our numerical method, and future plans for using and for releasing the code, please see our companion paper [15]. In this letter we will focus on the main result of these simulations: the first numerical demonstration of an inhomogeneous, but nearly FLRW, cosmological space time in full GR.

The BSSN Formalism: The BSSN formalism parameterizes the spacetime metric by

$$g_{\mu\nu} = \begin{pmatrix} -\alpha^2 + \gamma_{lk}\beta^l\beta^k & \beta_i \\ \beta_j & \gamma_{ij} \end{pmatrix} \quad (1)$$

where we generally refer to α as the ‘lapse’, and β_i as the ‘shift’. The metric is rescaled by a conformal factor, ϕ , so that $\gamma_{ij} = e^{4\phi}\bar{\gamma}_{ij}$, with $\det(\bar{\gamma}_{ij}) = 1$. The components of the 3-metric are then dynamically evolved for a particular gauge choice, along with the extrinsic curvature K_{ij} . To do this latter part, the extrinsic curvature is decomposed into a trace part, K , and a conformally related trace-free part, \bar{A}_{ij} , via $K_{ij} = e^{4\phi}\bar{A}_{ij} + \frac{1}{3}\gamma_{ij}K$, whose indices are raised and lowered by the conformal metric.

The content of the Universe is decomposed into,

$$\rho = n_\mu n_\nu T^{\mu\nu} \quad (2)$$

$$S_i = -\gamma_{i\mu} n_\nu T^{\mu\nu} \quad (3)$$

$$S_{ij} = \gamma_{i\mu} \gamma_{j\nu} T^{\mu\nu}, \quad (4)$$

where $T^{\mu\nu}$ is the stress-energy tensor, $n_\mu = (-\alpha, \vec{0})$ and $S = \gamma^{ij} S_{ij}$. (For a full textbook treatment, see eg. [16].)

The dynamical equations of motion for the metric are determined by Einstein's equations; however, for stability the auxiliary conformal connection variables $\bar{\Gamma}^i$ are evolved simultaneously in order to eliminate terms with mixed derivatives when calculating the Ricci tensor. While COSMOGRAPH allows for arbitrary lapse and shift (see [15]), in this letter we employ synchronous gauge (geodesic slicing). In this gauge the lapse is a fixed constant ($\alpha = 1$), and there is no shift ($\beta^i = 0$). The system we evolve is

$$\partial_t \phi = -\frac{1}{6} K \quad (5)$$

$$\partial_t \bar{\gamma}_{ij} = -2\bar{A}_{ij} \quad (6)$$

$$\partial_t K = \bar{A}_{ij} \bar{A}^{ij} + \frac{1}{3} K^2 + 4\pi(\rho + S) \quad (7)$$

$$\partial_t \bar{A}_{ij} = e^{-4\phi} (R_{ij} - 8\pi S_{ij})^{TF} + K \bar{A}_{ij} - 2\bar{A}_{il} \bar{A}_j^l \quad (8)$$

$$\partial_t \bar{\Gamma}^i = 2\bar{\Gamma}_{jk}^i \bar{A}^{jk} - \frac{4}{3} \bar{\gamma}^{ij} \partial_j K - 16\pi \bar{\gamma}^{ij} S_j + 12\bar{A}^{ij} \partial_j \phi. \quad (9)$$

For a flat FLRW solution to Einstein's equations, the BSSN variables can be directly translated to FLRW variables. The spatial metric is $\gamma_{ij} = a^2 \delta_{ij}$, meaning $\gamma \equiv \det \gamma_{ij} = a^6$. This relationship, along with our gauge choice, gives us a translation between BSSN and FLRW parameters: $H \sim -\frac{1}{3} K$ and $a \sim \gamma^{1/6} = e^{2\phi}$.

As a proxy for a universe containing matter, we source the metric with a flux-conservative form of the relativistic hydrodynamic equations [17]. In this letter, we restrict ourselves to a $w = 0$ cosmological fluid with rest-mass density ρ_0 and no initial velocity component; the contribution to the source terms are then $\rho = \rho_0$, $S_i = 0$ and $S_{ij} = 0$ (and so also $S = 0$). The equation of motion for the matter fluid in the absence of initial velocity and for our gauge choice is a simple conservation law,

$$\partial_t \tilde{D} = \partial_t (\gamma^{1/2} \rho_0) = 0. \quad (10)$$

We evolve a finite-volume 3-torus universe with periodic boundary conditions. We set the total volume of the simulation such that the length of any side, $L = n H_I^{-1} = N \Delta x$, is an arbitrary fraction, n , of the (initial) cosmological horizon in an exact FLRW solution, H_I^{-1} . Working in units of H_I then fixes the initial energy density of the corresponding FLRW solution to

$$\rho_{FLRW} = \frac{3}{8\pi} \left(\frac{n}{N} \right)^2. \quad (11)$$

In all of the simulations presented in this letter, we take $n = 1/2$, Δx is the coordinate distance between points and our units of momentum are $\Delta k = 2\pi/L$.

Initial Conditions: The initial surface from which we evolve should satisfy the Hamiltonian and momentum constraint equations,

$$\mathcal{H} \equiv \bar{\gamma}^{ij} \bar{D}_i \bar{D}_j e^\phi - \frac{e^\phi}{8} \bar{R} + \frac{e^{5\phi}}{8} \bar{A}_{ij} \bar{A}^{ij} - \frac{e^{5\phi}}{12} K^2 + 2\pi e^{5\phi} \rho = 0 \quad (12)$$

and

$$\mathcal{M}^i \equiv \bar{D}_j (e^{6\phi} \bar{A}^{ij}) - \frac{2}{3} e^{6\phi} \bar{D}^i K - 8\pi e^{10\phi} S^i = 0. \quad (13)$$

For an FLRW solution, the Hamiltonian constraint is one of the Friedman equations, and all terms in the momentum constraint equation are zero.

Solving Eqs. 12 and 13 for an arbitrary matter source does not uniquely specify a spatial metric; unconstrained degrees of freedom remain. Making choices that simplify the constraint equations, such as using the conformal transverse-traceless decomposition, can make finding an initial surface easier. Rather than attempting to set initial conditions that perfectly mimic our universe, we opt to obtain a simple solution to Eq. 12 that is approximately a power-law in momentum space at large and small wavevector k , and peaks at a desired scale.

We first specify an extrinsic curvature (akin to the Hubble parameter) approximately determined by the average density, corresponding to an FLRW background. We then introduce fluctuations in the matter field and conformal factor, approximately setting the matter density power spectrum up to that conformal factor. At large scales (small k) the matter power spectrum we choose scales as $P_k \propto k$, and at small scales (large k) as $P_k \propto k^{-3}$ [18]. Given a peak scale k_* and corresponding peak amplitude P_* , the conformally related matter power spectrum (and approximate matter power spectrum) is then

$$P_k^\rho = \frac{4P_*}{3} \frac{k/k_*}{1 + \frac{1}{3}(k/k_*)^4}. \quad (14)$$

Again, note that this is not intended to perfectly represent our universe, and issues of gauge and conformal rescalings have not been addressed. Also significantly, we introduce a cutoff k_{cutoff} in order to reduce fluctuations on scales where grid effects become important, so that fluctuations are resolved by sufficiently many points. The spectrum is cut using a sigmoid,

$$P_k^{\text{cutoff}} = \frac{1}{1 + \exp[10(k - k_{\text{cutoff}})]} P_k. \quad (15)$$

In this work we take k_{cutoff} to be $10\Delta k$ so that on a $N^3 = 128^3$ grid we resolve the shortest wavelengths with 12 grid points for our initial conditions. We find excessive constraint violation for larger cutoffs [15].

We construct the initial metric by decomposing ρ into ρ_K , which sources the trace of the extrinsic curvature K , and ρ_ψ , which sources the conformal factor $\psi \equiv e^\phi$. The total density is $\rho = \rho_K + \rho_\psi$. We use a conformally flat metric ($\bar{\gamma}_{ij} = \delta_{ij}$) and set the trace-free part of the extrinsic curvature to zero, leaving us with two more simple equations to solve:

$$\nabla^2 \psi = -2\pi\psi^5 \rho_\psi \quad (16)$$

$$K = -\sqrt{24\pi\rho_K}. \quad (17)$$

Here we choose K to be constant on the initial slice. The nonlinear equation for ψ is then difficult to solve for a fixed matter source, with attempted relaxation and iterative solution methods tending to find the $\psi = 0$ solution. We therefore create a Gaussian-random realization of the field ψ with a power spectrum $P_k^\psi = P_k^\rho/k^4$, and then solve for ρ . Note that ρ_K is not necessarily the average density, as ρ_ψ can have nonzero average (although the average of $\psi^5 \rho_\psi$ must be zero for periodic boundary conditions).

In more conceptual terms, we parameterize the spatial distortion of the metric at each point in terms of two parameters. ϕ holds information about the volume at that point, $\gamma^{1/2} = e^{6\phi}$; K encodes the rate at which that volume is changing, $\gamma^{-1/2} d\gamma^{1/2}/\Delta t = 3K$. For a given distribution of matter ρ , one has physical (not just gauge) freedom to chose a specific solution for the (initial) values of ϕ and K . In the FLRW limit, ϕ increases monotonically, and $\phi - \phi_{\text{initial}}$ corresponds to half the number of elapsed e-foldings, $a_{\text{FLRW}} = e^{2\phi_{\text{FLRW}}}$. We therefore use the spatial average value, $\bar{\phi}$, as a proxy for time in most of our plots, which is certainly a good choice if we are close to the FLRW solution.

We have examined the accuracy of our model by looking at how well we satisfy the two main constraint equations. Numerically, we employ a constraint damping term [19] to reduce the amount of constraint violation, although it has no significant effect on the quantities of interest in the short term. Details can be found in [15].

Results: Having set initial conditions describing a universe expanding at a constant rate across a set of points, each representing slightly different volumes, we can address our two initial questions. The first of these addresses how well FLRW quantities are recovered in our analysis. To test this we compare the average value of K and ρ . In an exact FLRW universe, $K = -\sqrt{24\pi\rho}$. We have chosen a large amplitude of inhomogeneity σ_ρ/ρ , but one low enough that no point has a negative ρ in the initial conditions. In the code we set a value of P_* – which maps directly to the variation of the density parameter, $\sigma_\rho/\bar{\rho}$. Fig. 1 shows that for $\sigma_\rho/\bar{\rho} = 0.05$, we see excellent agreement with FLRW cosmology for averaged quantities.

If inhomogeneities are important in our volume, we expect that varying the value of $\sigma_\rho/\bar{\rho}$ should induce in-

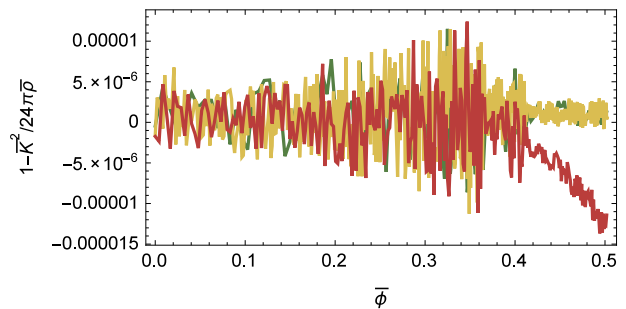


FIG. 1: A comparison of the average value of K for three different resolutions (64^3 red, 128^3 green, and 256^3 yellow) versus the average value of the conformal factor, $\bar{\phi}$. This simulation has inhomogeneities with $\sigma_\rho/\bar{\rho} = 0.05$.

creasingly important variations in K . Fig. 2 shows the reaction of the simulation to values of $\sigma_\rho/\bar{\rho}$ between about 2% and 10%. We see that σ_K/\bar{K} grows over the course of the simulations.

It is, however, evidence of growth of inhomogeneities *beyond a linear approximation* that is the main result of this paper. Even for relatively small variance in the matter field, $\mathcal{O}(5\%)$ deviations from linear expectations emerge. This is clear in fig. 2 (right panel) which shows how the local response to the metric is related to local over(under)densities.

We can attach some intuition to this result. We can analytically predict the metric to linear order in perturbations δK and $\delta\rho$ around average quantities $\bar{\rho}$ and \bar{k} , by writing down the evolution equations

$$\partial_t \delta\rho = \bar{\rho} \delta K + \bar{K} \delta\rho \quad (18)$$

$$\partial_t \delta K = \frac{2}{3} \bar{K} \delta K + 4\pi \delta\rho. \quad (19)$$

These are simple ODEs. Indeed, so long as any contribution from $\tilde{A}_{ij} \tilde{A}^{ij}$ is negligible, even the full evolution equations for ρ and K remain a set of ODEs that can be integrated easily. The dashed lines in the right panel of Fig. 2 show the behavior of solutions to these equations for our initial conditions. The curves show that the response of the metric is centered about the linear-order predicted value, but exhibit noticeable deviations from it.

While we have so far demonstrated that we generate variations of the extrinsic curvature, K , from point to point, we would like to conclude by doing a more clearly gauge-invariant test. One of the main predictions of an FLRW universe is that any path on a constant t surface (no matter the shape) has a proper length that scales with the scale factor of the Universe. In our simulations we will define a set of arbitrary paths on our constant t hyper-surfaces. If we calculate the proper length of these paths and track the ratio of these lengths as a function of time, we can tell whether we are truly seeing deviations from FLRW behavior. Fig. 3 shows that the growth of

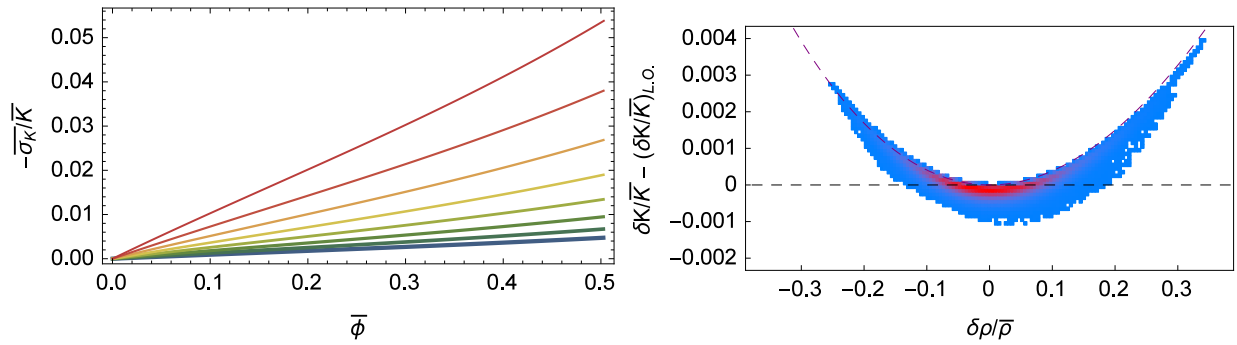


FIG. 2: The left panel shows variations in the extrinsic curvature, σ_K/\bar{K} , versus variations in $\sigma_\rho/\bar{\rho}$ over the course of a number of runs. The initial $\sigma_\rho/\bar{\rho}$ for these runs were $\sigma_\rho/\bar{\rho} = 0.009, 0.0133, 0.019, 0.027, 0.038, 0.053, 0.076$, and 0.107 from bottom to top, or blue to red. The right panel shows the relationship between fluctuations in matter density and extrinsic curvature at $\bar{\phi} = 0.5$ (one e-fold) as differences from a linear approximation. The black dashed line represents the linear-order analytic solution, dashed purple the solution excluding $\tilde{A}_{ij}\tilde{A}^{ij}$ contributions, and binned data from a simulation corresponding to an intermediate value of inhomogeneity, $\sigma_\rho/\bar{\rho} = 0.038$. We see local violations of the linear-order approximation of $\mathcal{O}(5\%)$.

the proper length of these paths depends on the length of the path (and not just some scale factor, a). Further, Fig. 3 suggests that this departure is more important at smaller distances than at larger distances.

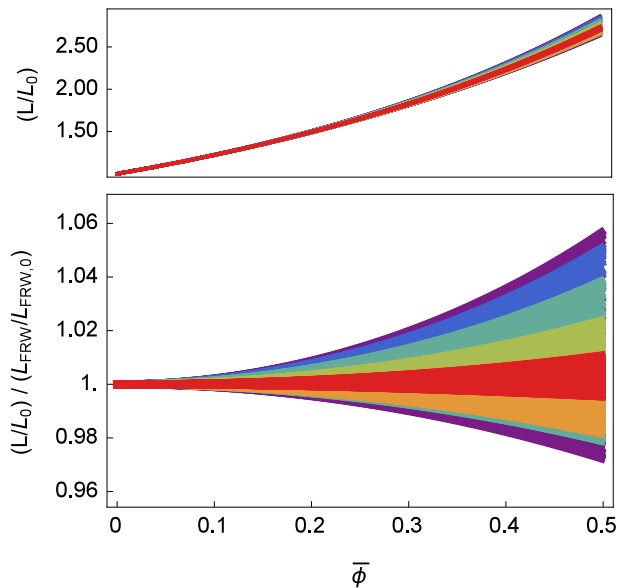


FIG. 3: The top panel shows ratio of the proper length to the initial length of six sets of 2^7 paths in our simulation. The color coding goes from paths of initial coordinate distance of $4\Delta x$ (purple) to paths of initial coordinate distance $128\Delta x$ (red) in spectral order. The bottom panel shows the same set paths, but compares the ratio of proper length to initial proper length with the FLRW estimate. We note that shorter paths deviate more from the FLRW expectation.

Discussion: We have seen that the conformal-scaling factor varies on sub-horizon scales. These local variations indicate that non-linear gravitational effects are present on cosmological scales. While this should not be surpris-

ing, this is the first quantified study of the expansion of an inhomogeneous near-FLRW spacetime within a fully General Relativistic framework. We further show that this effect is a truly physical one, and that the proper distances between points do not quite obey FLRW rules.

Our companion paper [15] provides further details on our numerical methods and the numerical tests to which we have subjected our code, COSMOGRAPH. In future work we expect to report on improved code performance near FLRW solutions, and to quantify the effects on standard physical observables, such as understanding how photons respond to non-linear gravitational effects in an inhomogeneous universe.

Acknowledgments We would like to thank Eugene Lim, Katy Clough, and Thomas Baumgarte for valuable conversations that contributed to this project. JTG is supported by the National Science Foundation, PHY-1414479; JBM and GDS are supported by a Department of Energy grant DE-SC0009946 to the particle astrophysics theory group at CWRU. We acknowledge the National Science Foundation, the Research Corporation for Science Advancement and the Kenyon College Department of Physics for providing the hardware used to carry out some of these simulations. This work also made use of the High Performance Computing Resource in the Core Facility for Advanced Research Computing at Case Western Reserve University.

-
- [1] F. Pretorius, Phys. Rev. Lett. **95**, 121101 (2005), gr-qc/0507014.
 - [2] M. Campanelli, C. O. Lousto, P. Marronetti, and Y. Zlochower, Phys. Rev. Lett. **96**, 111101 (2006), gr-qc/0511048.
 - [3] J. G. Baker, J. Centrella, D.-I. Choi, M. Koppitz, and J. van Meter, Phys. Rev. Lett. **96**, 111102 (2006), gr-qc/0511048.

- qc/0511103.
- [4] K. Clough, P. Figueras, H. Finkel, M. Kunesch, E. A. Lim, and S. Tunyasuvunakool (2015), 1503.03436.
 - [5] M. C. Babiuc et al., *Class. Quant. Grav.* **25**, 125012 (2008), 0709.3559.
 - [6] A. Paranjape (2009), 0906.3165.
 - [7] T. Clifton and P. G. Ferreira, *Phys. Rev.* **D80**, 103503 (2009), [Erratum: *Phys. Rev.* D84,109902(2011)], 0907.4109.
 - [8] T. Clifton and P. G. Ferreira, *JCAP* **0910**, 026 (2009), 0908.4488.
 - [9] T. Clifton, P. G. Ferreira, and K. O'Donnell, *Phys. Rev.* **D85**, 023502 (2012), 1110.3191.
 - [10] K. Bolejko and P. G. Ferreira, *JCAP* **1205**, 003 (2012), 1204.0909.
 - [11] T. Clifton, D. Gregoris, K. Rosquist, and R. Tavakol, *JCAP* **1311**, 010 (2013), 1309.2876.
 - [12] T. W. Baumgarte and S. L. Shapiro, *Phys. Rev.* **D59**, 024007 (1999), gr-qc/9810065.
 - [13] M. Shibata and T. Nakamura, *Phys. Rev.* **D52**, 5428 (1995).
 - [14] R. L. Arnowitt, S. Deser, and C. W. Misner, *Phys. Rev.* **116**, 1322 (1959).
 - [15] J. B. Mertens, J. T. Giblin, and G. D. Starkman (2015), 1511.01106.
 - [16] T. W. Baumgarte and S. L. Shapiro, *Numerical Relativity: Solving Einstein's Equations on the Computer* (Cambridge University Press, Cambridge, UK, 2010).
 - [17] J. A. Font, *Living Rev. Rel.* **3**, 2 (2000), [Living Rev. Rel.6,4(2003)], gr-qc/0003101.
 - [18] M. Tegmark et al. (SDSS), *Phys. Rev.* **D69**, 103501 (2004), astro-ph/0310723.
 - [19] M. D. Duez, S. L. Shapiro, and H.-J. Yo, *Phys. Rev.* **D69**, 104016 (2004), gr-qc/0401076.